

Integrating micromagnets and hybrid nanowires for topological quantum computing

Malcolm J. A. Jardine,¹ John P. T. Stenger,¹ Yifan Jiang,¹ Eline J. de Jong,² Wenbo Wang,³ Ania C. Bleszynski Jayich,³ and Sergey M. Frolov¹

¹*Department of Physics and Astronomy, University of Pittsburgh, Pittsburgh, PA, 15260, USA*

²*Department of Applied Physics, Eindhoven University of Technology, 5600 MB Eindhoven, The Netherlands*

³*Department of Physics, University of California, Santa Barbara CA 93106, USA*

Majorana zero modes are expected to arise in semiconductor-superconductor hybrid systems, with potential topological quantum computing applications. One limitation of this approach is the need for a relatively high external magnetic field that should also change direction at nanoscale. This proposal considers devices that incorporate micromagnets to address this challenge. We perform numerical simulations of stray magnetic fields from different micromagnet configurations, which are then used to solve for Majorana wavefunctions. Several devices are proposed, starting with the basic four-magnet design to align magnetic field with the nanowire and scaling up to nanowire T-junctions. The feasibility of the approach is assessed by performing magnetic imaging of prototype patterns.

I. INTRODUCTION

One-dimensional topological superconductors host Majorana zero modes (MZMs) [1, 2]. They are promising for fault-tolerant quantum computing because of the predicted topological protection that they facilitate [3, 4]. While there has been considerable effort applied to identify MZMs in semiconductor nanowires [5–7], the evidence to date is not conclusive due to plausible alternative explanations such as non-topological Andreev Bound States [8, 9]. With new developments in materials research and experimental methods it is reasonable to expect that the present day challenges can be overcome [10]. We look beyond to explore how generating local magnetic fields using micromagnets can aid in the design of Majorana devices.

There have been several studies on incorporating magnetic materials to induce MZM in hybrid systems, though the questions asked were different. One class of ideas has focused on generating synthetic spin-orbit coupling in weak spin-orbit materials through nanomagnet patterning [11–18]. Another class imagines shells of magnetic insulators on nanowires as a path to topological superconductivity through using exchange interactions [19, 20]. These results have sparked a debate about the feasibility and true origin of the observed signals [21–24].

In this work we propose how stray magnetic fields can be used to realize basic two-Majorana building blocks, as well as four-Majorana fusion and six-Majorana T-junction braiding devices. In the basic building block (Dragonfly, Fig. 1), four micromagnets are arranged around the nanowire such that field lines flow along the wire for 700 nm. We find through modular micromagnetics and Schrodinger calculations that it should be possible to enter the topologically superconducting state and achieve partial Majorana separation. Higher stray fields, e.g. from stronger or thicker magnets, would make the regime more robust. We perform magnetic force microscopy on prototype micromagnet patterns and find that it is possible to realize the building block Dragonfly

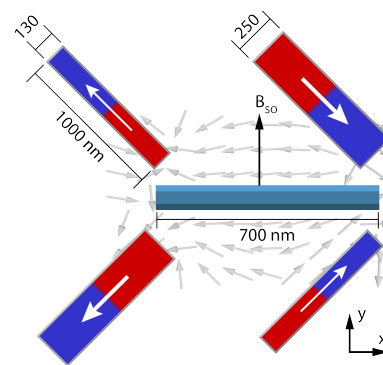


FIG. 1. The Dragonfly setup with four micromagnets (blue/red) and an overlay of the magnetic field calculated with MuMax3 (gray arrows). The nanowire runs horizontally with the spin-orbit axis vertical, indicated by B_{so} .

configurations, though arranging all micromagnets in a T-junction to the desired orientations will require very accurate control of switching fields.

II. NUMERICAL RESULTS

a. Brief Methods The micromagnetic simulation software MuMax3 [25] is used to simulate realistic single domain-sized micromagnets, including hysteretic magnetization and stray fields. Hysteresis simulations are performed to obtain the required magnetization state. Stray magnetic fields are integrated over the hexagonal nanowire cross-section to obtain a one-dimensional field profile. The field profile is used as input into a basic one-dimensional Majorana nanowire model [26] to obtain the energy spectrum and calculate Majorana wavefunctions γ_1 and γ_2 .

b. Dragonfly setup The setup presented in Fig. 1 is our basic configuration. The four micromagnets, that resemble a dragonfly, induce field lines along the nanowire, coming in at the right end, and flowing out of the left

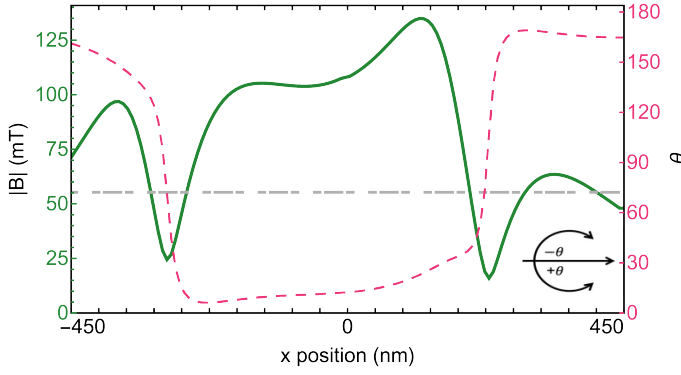


FIG. 2. Magnetic field profile, as a function of position, of the four magnet Dragonfly setup. Solid line is field amplitude and dashed line is field angle θ . The field is averaged over a hexagonal cross-section of the nanowire with a characteristic dimension of 100 nm. The horizontal dashed gray line indicates a uniform field for entering the topological regime.

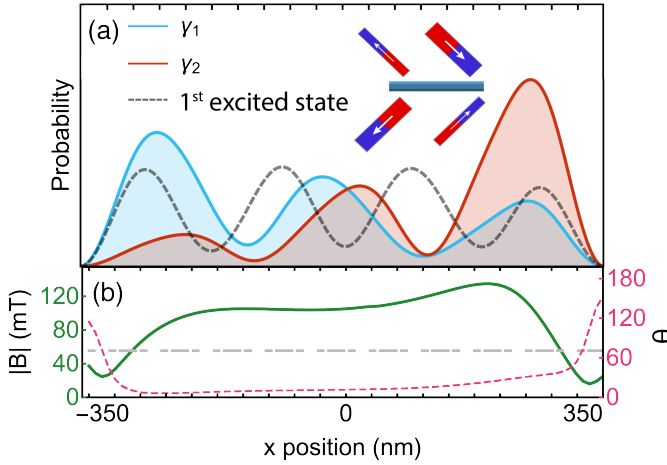


FIG. 3. (a) Probability distributions for two Majorana wavefunctions γ_1 and γ_2 . The first excited state (dashed line) is a bulk nanowire state. (b) Magnetic field profile reproduced from Fig. 2.

end. The field does not deviate by more than 30° over a 700 nm long nanowire segment, see Fig. 2. The relatively parallel field profile is required for MZMs formation, since such field is mostly orthogonal to the effective spin-orbit field, B_{so} [1, 2]. Four, rather than two, magnets are required to cancel y-fields and enhance x-fields. Micromagnets placed parallel to the nanowire, e.g. as a shell around the nanowire, produce largely y-fields that are highly non-uniform, concentrated outside the poles of the magnets [19].

The micromagnet widths are different to ensure different switching fields and to aid in the preparation of a desired mutual magnetization pattern [27]. The magnets are rotated at 45 degrees to aid magnetization through the hysteresis simulation. Magnets on opposite sides of the nanowire are perpendicular, and therefore the ex-

ternal field used for magnetization is also perpendicular for the pairs of magnets. The out of plane direction (z-component) of the simulated field is insignificant due to the symmetry of the micromagnet arrangement (see supplementary information).

Given the simulated magnetic field profile along the nanowire, there is clear Majorana polarization of the two MZMs, γ_1 and γ_2 , shown in Fig. 3. Though we assume a relatively low magnetic field for the topological transition, 50 mT. The two Majorana wavefunctions are highly overlapping. The lowest (partially separated Majorana) and the first excited energy levels have energies $E_0/\Delta = 0.28$ and $E_1/\Delta = 0.82$, where Δ is the superconducting gap. We note that a small global external field can be applied to boost Zeeman energy.

c. Double Dragonfly The next device (inset Fig. 4) combines two Dragonfly set-ups and an additional vertical magnet (dashed border), elongating the topological nanowire region. The concept can be repeated multiple times to further extend Majorana separation or create multiple pairs of MZM, for instance in Majorana fusion experiments [4]. The right Dragonfly unit is reflected: this means magnetic fields point opposite in the left and right nanowire segments. Nevertheless, left and right MZM form a pair due to field rotation provided by the central magnet. Using the same topological criterion we now find a more substantial MZM polarization of the ground state E_0 (red/blue), as it has little weight in the bulk. This is because the total length of the device is increased compared with the basic Dragonfly setup. The first excited state state (black-dashed) is mainly in the bulk as expected from a trivial bulk state. Application of an external field (10's of mT) in the positive y-direction in this case aligns the total field closer with the nanowire. Supplementary information presents other versions of the double Dragonfly.

d. T-junction braiding device The T-junction setup, shown in Fig. 5, explores how micromagnets could be used to realize a MZM braiding setup. The horizontal left and right arm sections are made by chaining together Dragonflies, and a perpendicular leg section in the middle has a micromagnetic configuration similar to a Dragonfly. This allows the field to be parallel to the nanowire in perpendicular sections of the wire, something that is not possible in a uniform external field.

The simulated stray field (supplementary Fig. S5a), with an additional small y-direction external magnetic field of around 40 mT, allowed MZMs to separate or couple across any two sections of the T-junction nanowire, seen in Fig. 6, where each arm of the junction has an electrostatic gate, G_1 , G_2 and G_3 , to control which sections are connected and disconnected.

With all three gates activated, we see three pairs of MZM (red, green and blue) confined to separate wire segments (Fig. 6a). With gate G_3 cutting off the perpendicular leg section, Fig. 6b, the lowest energy state (red) is localized at the ends of the top wire, demonstrating that the micromagnets allow this to act as a single,

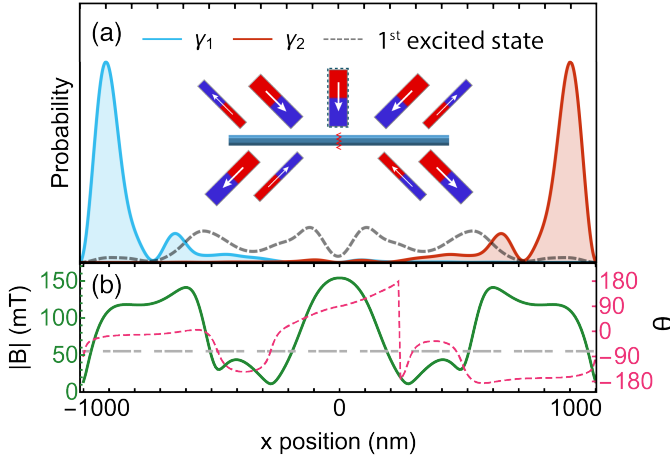


FIG. 4. (a) Probability distributions of two lowest energy states for double Dragonfly setup with gate open (shown in inset). MZM (red/blue) with $E_0/\Delta = 5.1 \times 10^{-4}$. The first excited state (grey dashed) with $E_1/\Delta = 1.6 \times 10^{-1}$. Inset: two dragonfly configurations, with zigzag indicating an electrostatic gate capable of dividing the nanowire in two parts. (b) Magnetic field profile along the wire, showing amplitude (solid) and angle (dashed).

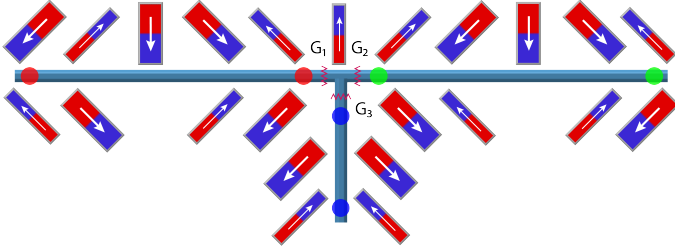


FIG. 5. T-Junction setup. The top two sections of nanowire are 5000 nm in length in total and the perpendicular section is 1100 nm. Zigzag lines indicate electrostatic gates. Circles indicate desired positions of 6 MZM with all gates on.

long topological superconductor. The second lowest energy state of the entire system is MZMs isolated in the perpendicular nanowire (blue), and the third lowest state (green) has weight mostly at the junction, representing two nearby MZM. We note that the fourth energy state is larger in energy with more weight in the bulk of the nanowire, suggesting it is not a partially hybridized MZM pair.

By activating gates G_1 or G_2 , Figs. 6c and 6d, we cut off either the left or the right section of nanowire. MZM states couple and decouple across the T-junction. These results suggest that a repeated Dragonfly setup could be used to realize a braiding setup, in principle, although with relatively complex micromagnet configurations.

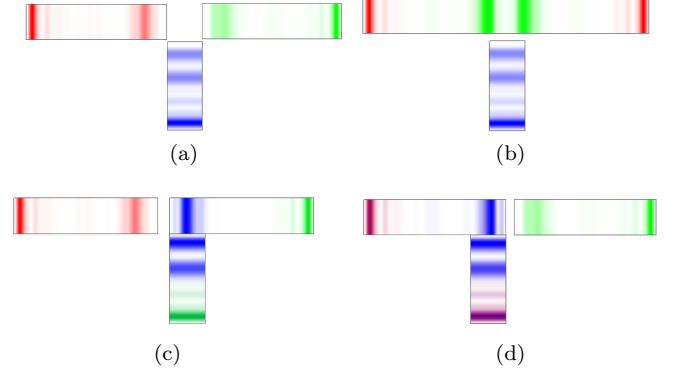


FIG. 6. Probability distributions (color) of the ground, second and third lowest energy with (a) all gates (b) gate G_3 , (c) gate G_1 , (d) gate G_2 activated. Colors chosen so that red wavefunction always has a weight on the left end. (a) The energies of the states are $E_0/\Delta = 1.6 \times 10^{-3}$ (red), $E_1/\Delta = 2.3 \times 10^{-3}$ (green), $E_2/\Delta = 9.4 \times 10^{-3}$ (blue), $E_3/\Delta = 1.5 \times 10^{-1}$ (not shown); (b) $E_0/\Delta = 1.6 \times 10^{-5}$ (red), $E_1/\Delta = 9.4 \times 10^{-3}$ (blue) and $E_2/\Delta = 4.2 \times 10^{-2}$ (green), $E_3/\Delta = 1.1 \times 10^{-1}$ (not shown). (c) $E_0/\Delta = 3.5 \times 10^{-4}$ (green), $E_1/\Delta = 1.6 \times 10^{-3}$ (red) and $E_2/\Delta = 4.3 \times 10^{-3}$ (blue), $E_3/\Delta = 1.3 \times 10^{-1}$ (not shown). (d) $E_0/\Delta = 7.2 \times 10^{-4}$ (red), $E_1/\Delta = 2.3 \times 10^{-3}$ (green) and $E_2/\Delta = 3.1 \times 10^{-3}$ (blue), $E_3/\Delta = 1.2 \times 10^{-1}$ (not shown).

III. MAGNETIC FORCE MICROSCOPY

We take the first step to evaluate these device concepts experimentally, by studying magnetization patterns of micromagnets. Ferromagnetic micro-strips are fabricated in a design that represents a simplified version of the braiding T-junction setup (Fig. 7). The design features three Dragonflies arranged in a T, and an extra vertical magnet. The strips are written by electron beam lithography (EBL) and the metal is deposited by electron beam evaporation from a CoFeB source (atomic ratio 30/55/15 before deposition) to a thickness of 20 nm. This is thinner than typical nanowires, and was done to reduce magnetic signal and permit higher resolution imaging. It is believed that the final strips are mostly CoFe without boron [28].

Magnetic force microscopy (MFM) and atomic force microscopy (AFM) are performed on triple Dragonflies (Fig. 7). An attempt is made to take advantage of hysteretic magnetization and prepare magnets preferentially in the desired Dragonfly configuration so that stray magnetic fields are along the imaginary nanowire in between the micromagnets. The range of field where wide and narrow micromagnets are antiparallel is determined from separate SQUID measurements to be between 15 and 20 mT, in agreement with Ref. [27], when reduced CoFe thickness is accounted for.

Twenty-four T-junctions with three Dragonflies each are imaged, and six of 76 total Dragonflies are magnetized as required for MZM generation. Fig. 7(b) shows one

such section with the magnetization marked by arrows (supplementary Fig. S8 shows all data). The occurrence of four micromagnets in the right orientation is consistent with random magnetization. While in our MuMax3 simulations it is possible to run through the hysteretic magnetization cycle and prepare micromagnets in the desired configuration, experimental variations in switching fields highlight a challenge. Optimized micromagnet fabrication will yield sharper switching and more reproducible switching fields in the future.

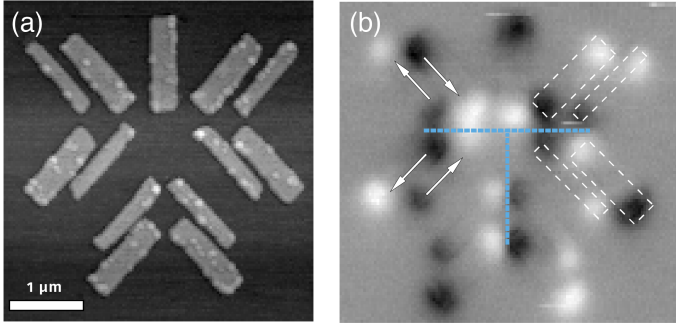


FIG. 7. (a) Atomic force microscopy (AFM) of a T-junction setup with three dragonfly magnet configurations. Magnetic film thickness is 20 nm. (b) Magnetic force microscopy (MFM) data on a different T-Junction of the same design. Arrows indicate magnetization direction, white dashed lines are example of magnet dimensions. Blue dashed line is where the Majorana nanowire is envisioned. The magnetic history was a magnetizing field from 100 mT to -16 mT to 0 mT applied at 45 degree direction, then 100 mT to -16 mT to 0 mT at 135 degrees.

IV. CONCLUSIONS, LIMITATIONS

We consider device concepts in which micromagnets generate stray field patterns suitable for the generation of Majorana zero modes. Our approach assumes micromagnets placed next to semiconductor nanowires that possess strong spin-orbit coupling, and are coated with superconducting shells. The requirements on the stray magnetic fields are that they are of sufficient strength to drive a topological transition, and should be oriented as much as possible along the nanowire. The building block of our magnetic design is a Dragonfly configuration in which four micromagnets are magnetized such that the magnetic field lines flow out of one pair of micromagnets, along the nanowire, and into the other pair (Fig. 1). By repeating the Dragonfly pattern along the nanowire, we can extend the length of the topological segment with addition of coupling magnets. The approach can also be

applied to T-junctions required for Majorana braiding experiments, in which case magnetic field turns into the T-junction leg that is perpendicular to the junction top.

Among the limitations is the still limited strength of stray fields from micromagnets. In previous experiments the typical stray fields are in the range of tens of milliTesla [27]. This is in principle sufficient to enter the topological regime in large g-factor semiconductor such as InSb nanowires, but it limits the parameter space for Majorana separation and manipulation. Stronger magnetic materials, or thicker micromagnets can help.

A challenge that became apparent from magnetic imaging of prototype structures is how to prepare all micromagnets in the appropriate relative magnetic orientation. This gets harder when the configurations become more complex such as for T-junctions. Though basic two-Majorana experiments should be possible already now, in the future better control over coercive fields, further pattern optimization, and direct magnetic writing can be deployed.

Among future ideas, a promising path is using a Y-junction instead of a T-junction [29], an approach that may require fewer micromagnets as some can be shared between the branches. Rather than gate-controlled MZM coupling, magnetic field mediated coupling can be investigated, by flipping micromagnets at the junctions. The implementation of the Poisson-Schrödinger equation to model MZM in the 3D geometry of a single nanowire could be integrated with 3D stray field profiles rather than simplified one-dimensional profiles integrated over the nanowire cross-section.

To summarize, nanoscale control over the field magnitude and direction is advantageous, particularly for advanced geometries where some nanowire segments may run perpendicular to others. Micromagnets could offer novel ways to control Majorana-based devices, for instance by switching magnetization in order to reposition or couple MZM.

Acknowledgements and funding. We thank S. Meynell and D. Yang for helpful discussions. Work in Pittsburgh (numerics and nanofabrication) supported by the Department of Energy DE-SC-0019274. A.B.J. acknowledges the support of the NSF Quantum Foundry through Q-AMASE-i program award DMR-1906325.

Code and data availability. Example MuMax3 scripts, numerical results data, Majorana simulation Mathematica notebooks are available on GitHub via <https://github.com/frolovgroup>.

Author Contributions. M.J. and E.J. performed MuMax3 simulations. M.J., E.J. and J.S. performed Majorana simulations. Y.J. fabricated micromagnet devices. W.W. and A.B.J. performed MFM/AFM imaging. M.J. and S.F. wrote the manuscript with input from co-authors.

-
- [1] Yuval Oreg, Gil Refael, and Felix von Oppen. Helical liquids and majorana bound states in quantum wires. *Phys. Rev. Lett.*, 105:177002, Oct 2010.
- [2] Roman M. Lutchyn, Jay D. Sau, and S. Das Sarma. Majorana fermions and a topological phase transition in semiconductor-superconductor heterostructures. *Phys. Rev. Lett.*, 105:077001, Aug 2010.
- [3] Sankar Das Sarma, Michael Freedman, and Chetan Nayak. Majorana zero modes and topological quantum computation. *npj Quantum Information*, 1(1):15001, 2015.
- [4] David Aasen, Michael Hell, Ryan V. Mishmash, Andrew Higginbotham, Jeroen Danon, Martin Leijnse, Thomas S. Jespersen, Joshua A. Folk, Charles M. Marcus, Karsten Flensberg, and Jason Alicea. Milestones toward majorana-based quantum computing. *Phys. Rev. X*, 6:031016, Aug 2016.
- [5] V. Mourik, K. Zuo, S. M. Frolov, S. R. Plissard, E. P. A. M. Bakkers, and L. P. Kouwenhoven. Signatures of majorana fermions in hybrid superconductor-semiconductor nanowire devices. *Science*, 336(6084):1003–1007, 2012.
- [6] S. M. Albrecht, A. P. Higginbotham, M. Madsen, F. Kuemmeth, T. S. Jespersen, J. Nygård, P. Krogstrup, and C. M. Marcus. Exponential protection of zero modes in majorana islands. *Nature*, 531(7593):206–209, 2016.
- [7] M. T. Deng, S. Vaitiekėnas, E. B. Hansen, J. Danon, M. Leijnse, K. Flensberg, J. Nygård, P. Krogstrup, and C. M. Marcus. Majorana bound state in a coupled quantum-dot hybrid-nanowire system. *Science*, 354(6319):1557–1562, 2016.
- [8] Eduardo JH Lee, Xiaocheng Jiang, Manuel Houzet, Ramón Aguado, Charles M Lieber, and Silvano De Franceschi. Spin-resolved andreev levels and parity crossings in hybrid superconductor-semiconductor nanostructures. *Nature nanotechnology*, 9(1):79–84, 2014.
- [9] P Yu, J Chen, M Gomanko, G Badawy, EPAM Bakkers, K Zuo, V Mourik, and SM Frolov. Non-majorana states yield nearly quantized conductance in proximitized nanowires. *Nature Physics*, pages 1–7, 2021.
- [10] S. M. Frolov, M. J. Manfra, and J. D. Sau. Topological superconductivity in hybrid devices. *Nature Physics*, 16(7):718–724, 2020.
- [11] Jelena Klinovaja, Peter Stano, and Daniel Loss. Transition from fractional to majorana fermions in rashba nanowires. *Phys. Rev. Lett.*, 109:236801, Dec 2012.
- [12] Jelena Klinovaja and Daniel Loss. Giant spin-orbit interaction due to rotating magnetic fields in graphene nanoribbons. *Phys. Rev. X*, 3:011008, Jan 2013.
- [13] Morten Kjaergaard, Konrad Wölms, and Karsten Flensberg. Majorana fermions in superconducting nanowires without spin-orbit coupling. *Phys. Rev. B*, 85:020503, Jan 2012.
- [14] MM Desjardins, LC Contamin, MR Delbecq, MC Dartailh, LE Bruhat, T Cubaynes, JJ Viennot, F Mallet, S Rohart, A Thiaville, et al. Synthetic spin-orbit interaction for majorana devices. *Nature materials*, 18(10):1060–1064, 2019.
- [15] Narayan Mohanta, Tong Zhou, Jun-Wen Xu, Jong E. Han, Andrew D. Kent, Javad Shabani, Igor Žutić, and Alex Matos-Abiague. Electrical control of majorana bound states using magnetic stripes. *Phys. Rev. Applied*, 12:034048, Sep 2019.
- [16] Stefan Rex, Igor V. Gornyi, and Alexander D. Mirlin. Majorana modes in emergent-wire phases of helical and cycloidal magnet-superconductor hybrids. *Phys. Rev. B*, 102:224501, Dec 2020.
- [17] Sara Turcotte, Samuel Boutin, Julien Camirand Lemyre, Ion Garate, and Michel Pioro-Ladrière. Optimized micromagnet geometries for majorana zero modes in low g -factor materials. *Phys. Rev. B*, 102:125425, Sep 2020.
- [18] L.N. Maurer, J.K. Gamble, L. Tracy, S. Eley, and T.M. Lu. Designing nanomagnet arrays for topological nanowires in silicon. *Phys. Rev. Applied*, 10:054071, Nov 2018.
- [19] Yu Liu, Saulius Vaitiekėnas, Sara Martí-Sánchez, Christian Koch, Sean Hart, Zheng Cui, Thomas Kanne, Sabbir A. Khan, Rawa Tanta, Shivendra Upadhyay, Martin Espiñeira Cachaza, Charles M. Marcus, Jordi Arbiol, Kathryn A. Moler, and Peter Krogstrup. Semiconductor-ferromagnetic insulator-superconductor nanowires: Stray field and exchange field. *Nano Letters*, 20(1):456–462, 01 2020.
- [20] S Vaitiekėnas, Y Liu, P Krogstrup, and CM Marcus. Zero-bias peaks at zero magnetic field in ferromagnetic hybrid nanowires. *Nature Physics*, 17(1):43–47, 2021.
- [21] Kim Pöyhönen, Daniel Varjas, Michael Wimmer, and Anton R Akhmerov. Minimal zeeman field requirement for a topological transition in superconductors. *arXiv preprint arXiv:2011.08263*, 2020.
- [22] Josias Langbehn, Sergio Acero Gonzalez, Piet W Brouwer, and Felix von Oppen. Topological superconductivity in tripartite superconductor-ferromagnet-semiconductor nanowires. *arXiv preprint arXiv:2012.00055*, 2020.
- [23] Aleksei Khindanov, Jason Alicea, Patrick Lee, William S Cole, and Andrey E Antipov. Topological superconductivity in nanowires proximate to a diffusive superconductor-magnetic insulator bilayer. *arXiv preprint arXiv:2012.12934*, 2020.
- [24] Maituo Yu, Saeed Moayedpour, Shuyang Yang, Derek Dardzinski, Chunzhi Wu, Vlad S. Pribiag, and Noa Marom. Dependence of the electronic structure of the eus/inas interface on the bonding configuration. *arXiv preprint arXiv:2104.01623*, 2021.
- [25] Arne Vansteenkiste, Jonathan Leliaert, Mykola Dvornik, Mathias Helsen, Felipe Garcia-Sanchez, and Bartel Van Waeyenberge. The design and verification of mumax3. *AIP Advances*, 4(10):107133, 2014.
- [26] John P. T. Stenger, Benjamin D. Woods, Sergey M. Frolov, and Tudor D. Stanescu. Control and detection of majorana bound states in quantum dot arrays. *Phys. Rev. B*, 98:085407, Aug 2018.
- [27] Y Jiang, E J de Jong, V van de Sande, S Gazibegovic, G Badawy, E P A M Bakkers, and S M Frolov. Hysteretic magnetoresistance in nanowire devices due to stray fields induced by micromagnets. *Nanotechnology*, 32(9):095001, dec 2020.
- [28] C. Bureau-Oxton. Fabrication de nanoaimants pour le contrôle rapide d’un spin électronique dans une boîte quantique double. *Université de Sherbrooke*, 2014.

- [29] Fenner Harper, Aakash Pushp, and Rahul Roy. Majorana braiding in realistic nanowire y-junctions and tuning forks. *Phys. Rev. Research*, 1:033207, Dec 2019.
- [30] A Yu Kitaev. Unpaired majorana fermions in quantum wires. *Physics-Uspekhi*, 44(10S):131–136, oct 2001.
- [31] Martin Leijnse and Karsten Flensberg. Introduction to topological superconductivity and majorana fermions. *Semiconductor Science and Technology*, 27(12):124003, nov 2012.
- [32] A. Manchon, H. C. Koo, J. Nitta, S. M. Frolov, and R. A. Duine. New perspectives for rashba spin–orbit coupling. *Nature Materials*, 14(9):871–882, 2015.
- [33] Georg W. Winkler, Andrey E. Antipov, Bernard van Heck, Alexey A. Soluyanov, Leonid I. Glazman, Michael Wimmer, and Roman M. Lutchyn. Unified numerical approach to topological semiconductor-superconductor heterostructures. *Phys. Rev. B*, 99:245408, Jun 2019.
- [34] Benjamin D. Woods, Tudor D. Stanescu, and Sankar Das Sarma. Effective theory approach to the schrödinger-poisson problem in semiconductor majorana devices. *Phys. Rev. B*, 98:035428, Jul 2018.
- [35] Jason Alicea, Yuval Oreg, Gil Refael, Felix von Oppen, and Matthew P. A. Fisher. Non-abelian statistics and topological quantum information processing in 1d wire networks. *Nature Physics*, 7(5):412–417, 2011.
- [36] John P. T. Stenger, Michael Hatridge, Sergey M. Frolov, and David Pekker. Braiding quantum circuit based on the 4π josephson effect. *Phys. Rev. B*, 99:035307, Jan 2019.

V. SUPPLEMENTARY INFORMATION

A. Background on Majorana nanowire model

MZMs are non-Abelian in nature and are their own antiparticle. They appear as topological, zero-energy states localized at the ends of a 1D system. They were first theoretically investigated in condensed matter systems by Kitaev in one-dimensional, spinless (p-wave), topological superconductors [30]. However, p-wave superconductors have yet to be realized experimentally, and, therefore, models that are experimentally accessible have been utilized in recent times. The prospect for MZMs that we are focused on is using semiconductor nanowire, superconductor hybrid systems in external magnetic fields [1, 2]. The hybrid systems utilize the nanowire's inherently strong spin-orbit coupling; proximity-induced s-wave superconductivity via contact with conventional superconductors; and the magnetic field to act as effective p-wave superconductors.

The Kitaev chain model is described by this Hamiltonian [30],

$$\hat{H}_p = -\mu \sum_i [c_i^\dagger c_i] - \frac{1}{2} \sum_i [tc_j^\dagger c_{j+1} + \Delta e^{i\phi} c_j c_{j+1} + H.c.] \quad (1)$$

where c_i destroys a spinless fermion at site i , c_i^\dagger creates a spinless fermion, μ is the chemical potential, $t > 0$ is the site hopping energy and $\Delta e^{i\phi}$ is the p-wave superconducting pairing term.

When this model is written in terms of Majorana fermion operators γ_1 and γ_2 , Kitaev showed that this describes a system with Majorana fermions that have on site and nearest neighbour interactions. The key insight was that in the topological regime when $|\mu| < t$, unpaired Majorana fermions are left at the ends of the 1D chain, which could be potentially detected and manipulated.

The semiconductor nanowire model is:

$$\hat{H}_{NW} = \left(\frac{p^2}{2m^*} - \mu + \alpha_R (\boldsymbol{\sigma} \times \mathbf{p}) \cdot \hat{\mathbf{z}} \right) \tau_z + V_z (\cos \theta \sigma_x + \sin \theta \sigma_y) + \Delta_s \tau_x \sigma_y \quad (2)$$

which acts on the Nambu spinor basis $\hat{\psi}_x = (c_{\uparrow x}, c_{\downarrow x}, c_{\uparrow x}^\dagger, -c_{\downarrow x}^\dagger)$. Here \mathbf{p} points along the nanowire in the x direction, Δ_s is the s-wave superconducting pairing term, $V_z = \frac{1}{2} g_{eff} \mu_B B$ is the Zeeman energy, θ is the angle of the field relative to the positive x-axis, τ and σ are Pauli matrices representing the particle-hole and spin spaces respectively, and α_R is the Rashba spin orbit coupling term. These parameters are taken constant because the nanowire is considered to be made of a homogeneous material. To be in the topological phase the following condition must be met

$$V_z > \sqrt{\mu^2 + \Delta_s^2} \quad (3)$$

When this system is deep in the topological phase it was shown that this reduces to a p-wave topological system described by Eq.(1). To simulate the model in a

finite one-dimensional system the continuum model is discretized on a 1D lattice in the electronic state basis, giving Eq. (4).

B. Further Reading

For basic introductory review of Majorana nanowire topic consider reading [31]. A perspective giving an explanation on Rashba spin-orbit coupling one can read [32]. Other relevant work on nanowires that deal with areas such as surface effects, effects of the contacts, electric field considerations, and try to comprehensively implement the model [26, 33]. For work that utilizes the Poisson Schrödinger equation to model MZMs in the 3D geometry of a single nanowire [26, 33, 34], where the use of 3D field profiles could give a better picture of systems in future studies. Further work on implementing micromagnets for use in Majorana based devices [27]. There are several different proposed braiding schemes using nanowire-network junction devices [26, 35], with options such as using local chemical potential changes [29] or flux gates [36].

C. Majorana Model Used

The implemented one-dimensional semiconductor-superconductor hybrid model is given by a discretized Hamiltonian,

$$\begin{aligned} \hat{H} = & \sum_n [(-\mu_n + \varepsilon_0) |n\rangle \langle n| \tau_z \otimes \sigma_0 \\ & + t(a) (|n+1\rangle \langle n| + H.c.) \tau_z \otimes \sigma_0 \\ & + \alpha(a) (|n+1\rangle \langle n| - H.c.) \tau_z \otimes (\boldsymbol{\sigma} \times \mathbf{p}) \cdot \hat{\mathbf{z}} \\ & + \tau_z \otimes V_{z,n} (\cos \theta_n \sigma_x + \sin \theta_n \sigma_y) |n\rangle \langle n| \\ & - \Delta_s \tau_x \otimes \sigma_x |n\rangle \langle n|], \end{aligned} \quad (4)$$

where

$$t(a) = \frac{\hbar^2}{2m^* a^2} \quad \alpha(a) = \frac{\alpha_R}{2a}. \quad (5)$$

The meaning and values used for the parameters are as follows. The momentum \mathbf{p} points in the direction of a section of nanowire, n labels the lattice site and τ and σ are Pauli matrices representing the particle-hole and spin spaces respectively. The s-wave superconducting pairing term is $\Delta_s = 0.08$ meV, the Rashba spin orbit coupling term $\alpha_R = 0.2$ eVÅ, effective electron mass $m^* = 0.04m_e$, and $g_{eff} = 50$ such as in InSb wires. Lastly, the Zeeman energy is $V_{z,n} = \frac{1}{2} g_{eff} \mu_B B_n$, with the magnetic field, B_n , and relative angle of the field to the x-axis, θ_n , being both site dependent and in general have a complicated structure due to the use of the micromagnets, a notable difference to many other works. The simulated magnetic field from MuMax3 is inputted

into the 1D nanowire-superconductor model via $V_{z,n}$, and the spectrum and eigenstates calculated via exact diagonalization. The effects of the non-uniform structure of the Zeeman energy were utilized and investigated by constructing longer devices with many micromagnets, and a T-junction set-up where perpendicular wires had different field directions.

Interpreting Majorana results. To investigate viability of the proposed devices, the MZMs signatures of state polarization and zero-energy pinning are required. A single electronic Majorana state, with energy E_0 , can be written in terms of the two Majorana wavefunctions via $\gamma_1 = c + c^\dagger$ and $\gamma_2 = -i(c - c^\dagger)$ and, due to the topological nature of MZMs, polarization of the two MZM will be apparent, seen as the localisation of two Majoranas at opposite ends of a single topological region of nanowire. In short systems the MZMs can be overlapping, and also could have a complicated structure due to the variation of the magnetic field or nanowire length. The first energy/excited state, denoted E_1 if there is a single pair of MZMs present, should have weight predominately in the bulk, with little overlap with the MZMs. The second signature is the near-zero energy of the MZM state, with good energy separation from the first energy state.

D. Micromagnetic Simulation Details

MuMax3 [25] is a GPU-accelerated micromagnetic simulation program that uses finite difference discretization methods, accurate sized magnetic domains within a single magnet for micro- to nano- scale system simulations, and was implemented to obtain the magnetic field used in the hybrid nanowire model. The micromagnets and nanowire structure are first constructed for each set-up in MuMax3, the requisite magnetization states achieved through hysteresis, if possible, and then the stray field is averaged over the hexagonal nanowire structure (such as InSb wires) with nanowire lengths ranging from half a micrometer to several micrometers and with diagonal width of 100 nm, typical of experiments. This field is then used in the Majorana model to show MZM signatures, with these calculations and hysteresis simulations determining the required final material properties, physical dimensions and positions of the micromagnet configuration. The code used for the calculations can be found on GitHub.

To obtain the required magnetization state, through hysteresis, the micromagnets start with many randomly orientated domains and then an external magnetizing field is applied and the system was relaxed at regular time intervals while ramping up and down the field. It was found that angling the micromagnets made obtaining the desired magnetization directions easier, as magnets on the opposite side of the nanowires were then perpendicular to each other. This allows the micromagnets to be closer together, however angling the magnets reduces the magnetic field, see Fig. S7, so these effects have to

be balanced to obtain the strongest magnetic field possible. The hysteresis process takes into account the material of magnets, which include saturation magnetization, anisotropy constants and exchange stiffness. One limitation present is the material of the nanowire, leads and other components were not taken into account in the simulation, but the main magnetic effects are presumed to come from the magnets themselves.

The magnetic material parameters of Cobalt are used due to several factors, first is that the constructed micromagnet devices are thought to be mainly composed of CoFe. Additionally, Cobalt is a common material used in the fabrication of micromagnets, and it allows for a relatively high saturation magnetization, and thus a stronger stray field, while also allowing for a reasonable coercive field due to Cobalt's exchange stiffness and cubic anisotropy constant. This allows for an appropriate demagnetization/stray field in the nanowire region, while also reliably obtaining the magnetization direction required for the setup, and additionally allowing for a small external field to be applied without accidentally flipping the magnets. The parameters used are a saturation magnetisation of 1.44×10^6 A/m, exchange stiffness 3.0×10^{-11} J/m, anisotropy constant K_1 4.5×10^5 , anisotropy constant K_2 1.5×10^5 and a Landau-Lifshitz damping constant of 0.01.

For the Dragonfly setup, the positions and dimensions of the set-up are as follows. Micromagnets of two different widths are reliable and sufficient enough for hysteresis and field production purposes, with the material properties chosen to be that of cobalt. The dimensions of all magnets in this work are either that of the thin magnet, with dimensions $130 \times 1000 \times 100$ nm, or the thick magnet with dimensions $250 \times 1000 \times 100$ nm, as the different sized magnets flip at different coercive fields. The magnets are rotated at 45 degrees to additionally aid the reliability of magnetization directions. The nanowire has a hexagonal cross-section, with a long diagonal length of 100 nm, and length of 700 nm so it spanned the region of parallel field from the magnets. The centers of the micromagnets are displaced from the middle of the nanowire to the left and right by 250 nm, with magnets of the different widths opposite each other. The y-displacement of the micromagnets from the nanowire is chosen such that the nearest corner of each magnet is 40 nm from the nanowire. These positions are one workable configuration, and changing the positions, dimensions or magnet material parameters will change the magnetic field profile, but that this is the optimal set-up found. We note it is difficult to obtain a field larger than ~ 150 mT in the current set-up, and additionally the superconducting gap is not necessarily fixed experimentally, which will change the field requirements.

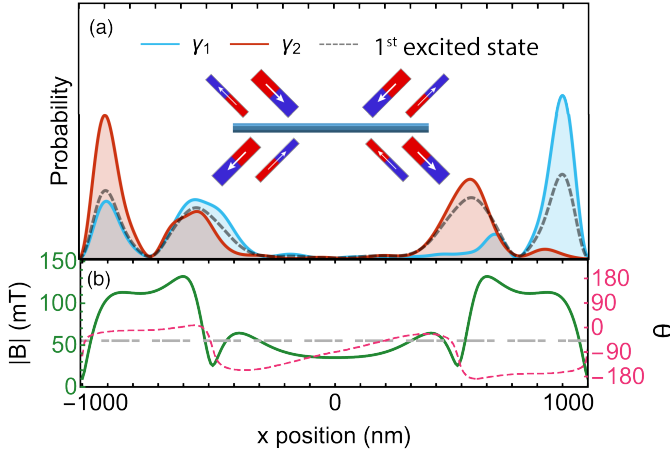


FIG. S1. (a) Probability distributions for two lowest energy states, this system shows two mixed/degenerate states with no clear Majorana polarization and no higher energy state being gapped out. The energies of both states $E_1/\Delta = 3.9 \times 10^{-2}$ and $E_2/\Delta = 4.6 \times 10^{-2}$. (b) Field profile along wire.

E. Supplementary Results

1. Double Dragonfly without extra magnet

This particular double Dragonfly device (inset Fig. S1(a)), is different from the one shown in the main text because it combines two individual Dragonfly set-ups (without the 9th magnet). The magnetic field has a large region of low magnitude field in the middle section, see bottom panel of Fig. S1(b). The eigenstate profiles and energy spectrum suggest there are two pairs of uncoupled MZM on each side of the wire.

2. Double Dragonfly with extra Magnet

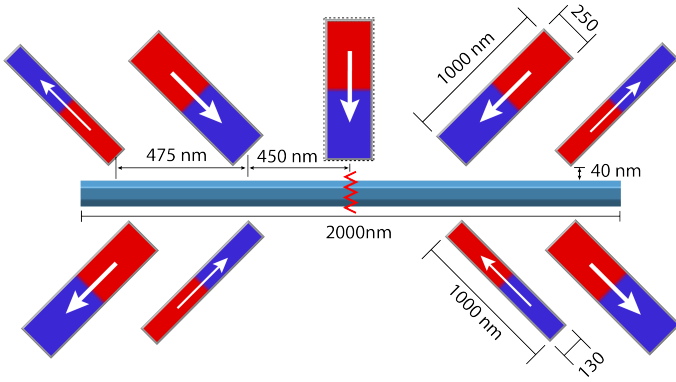


FIG. S2. The double Dragonfly setup with the magnet in the middle and a potential gate, dimensions given. Toggling this gate allows the left and right side of the wire to be coupled or uncoupled.

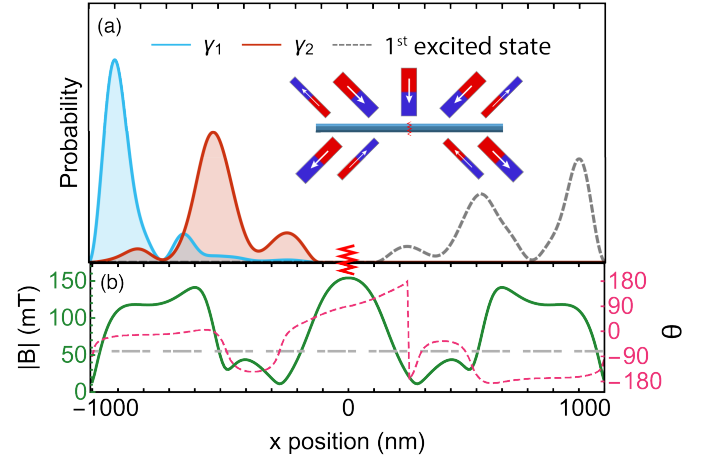


FIG. S3. (a) Probability distributions for two lowest energy states for double Dragonfly setup with the 9th magnet and the gate closed (inset). The probability distributions shows two separate pairs of MZMs in each section of the wire, the left is written in the Majorana basis with energy $E_1/\Delta = 3.1 \times 10^{-2}$ (red and cyan), and another pair in the right section in the electronic basis with energy $E_2/\Delta = 3.1 \times 10^{-2}$ (black- dashed line). The third state is well separated at $E_3/\Delta = 8.9 \times 10^{-1}$. (b) Field profile along wire.

Dimensions of the double Dragonfly with an extra magnet are given in Fig. S2. A gate is turned on in the middle region of the nanowire (Fig. S3 red zig-zag line), which causes the ends of nanowire to become uncoupled and four MZMs to appear. This is implemented as a large potential barrier spanning around 10 sites, and could be experimentally achieved by applying an external voltage, effectively cutting off different parts of the nanowire. There are two pairs of separate MZMs in each parallel region of field, similar to the single Dragonfly set-up, with similar energies of $E_0/\Delta = 3.1 \times 10^{-2}$ and $E_1/\Delta = 3.2 \times 10^{-2}$, and the first excited state being at a larger energy of $E_2/\Delta = 8.9 \times 10^{-1}$.

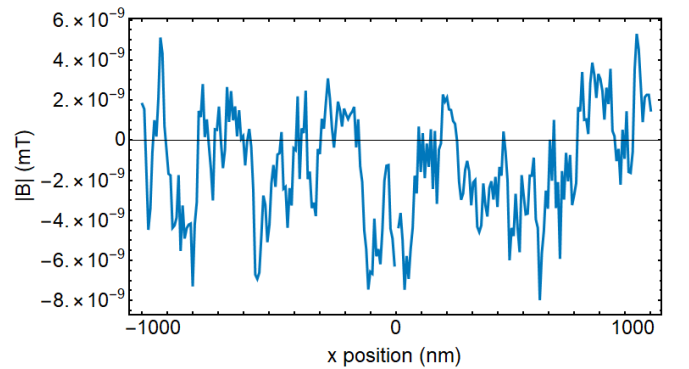


FIG. S4. B_z field component along the wire for the double Dragonfly with the middle ninth magnet. The B_z data for other set-ups available on GitHub.

3. *T-junction magnetic fields*

To construct the magnetic field profile the central triple Dragonfly section is simulated in MuMax3, and then the top field profile elongated by attaching two flipped copies of the top field profile and connecting these on the ends. The magnetic field in the top nanowire rotates smoothly across the length of the nanowire (see Fig. S5a), and the whole nanowire is one topological region. The perpendicular section of nanowire's magnetic field is similar to that of the single Dragonfly set-up, with a large parallel region of around 700 nm, this only points up due to the same width magnets being opposite each other, see Fig. S5b. Additionally, an external magnetic field of 40 mT in the y-direction is added to facilitate maximum coupling.

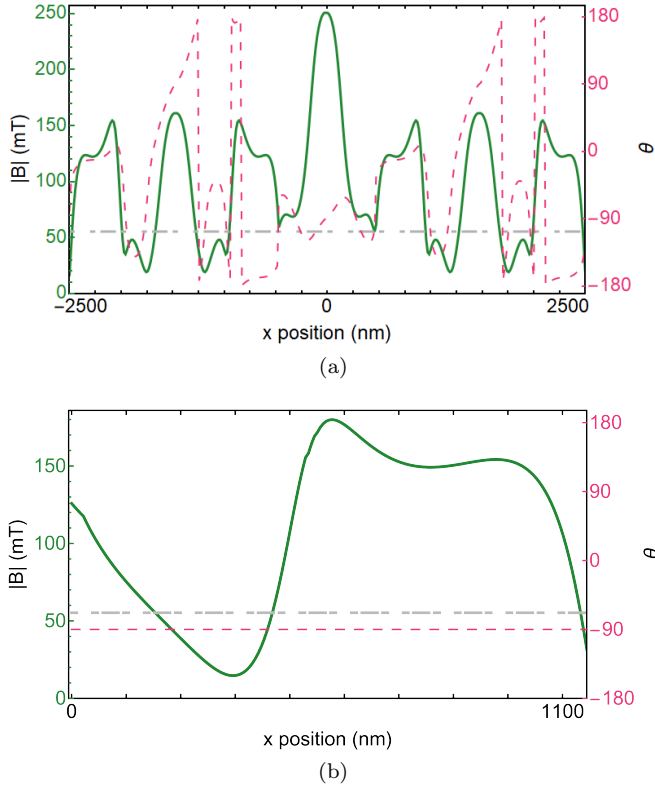


FIG. S5. (a) Magnetic field of top wire for T-Junction. (b) Magnetic field in the T-Junction leg (vertical segment of nanowire).

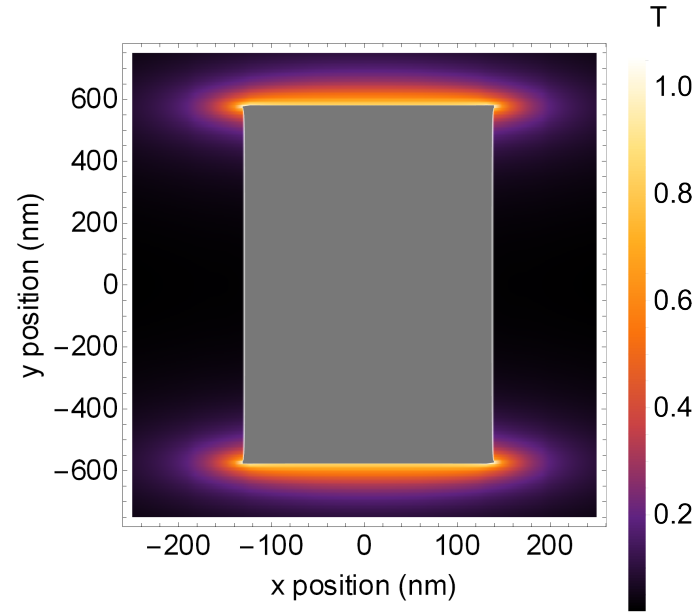


FIG. S6. Magnitude heat map for a 2D slice through the middle (50nm) of a micromagnet of dimensions 230X1000X100 nm. Note the field is very weak away from the micromagnet ends.

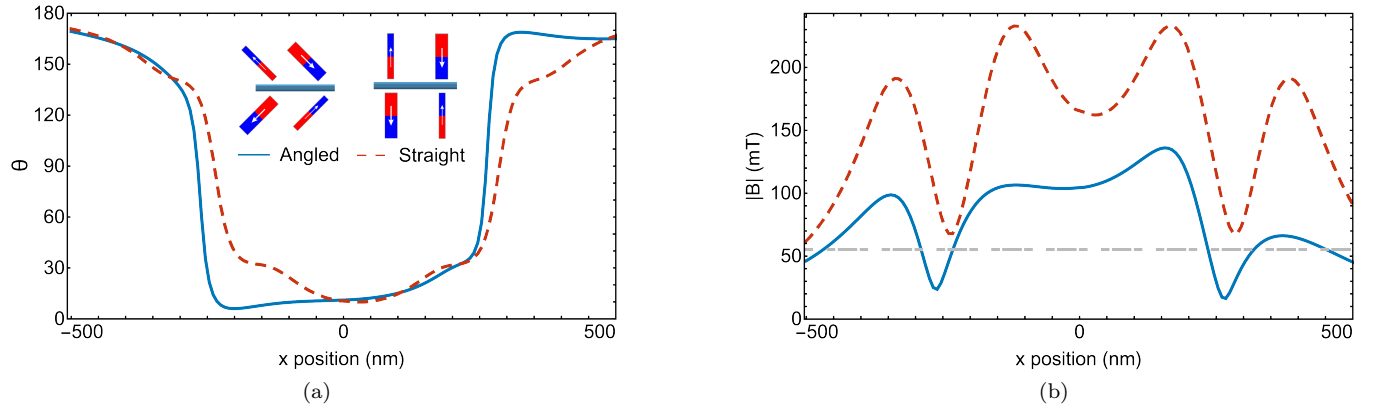


FIG. S7. This compares the a rotated and un-rotated Dragonfly configuration. The solid line is the rotated set-up and the dashed line is the straight set-up.

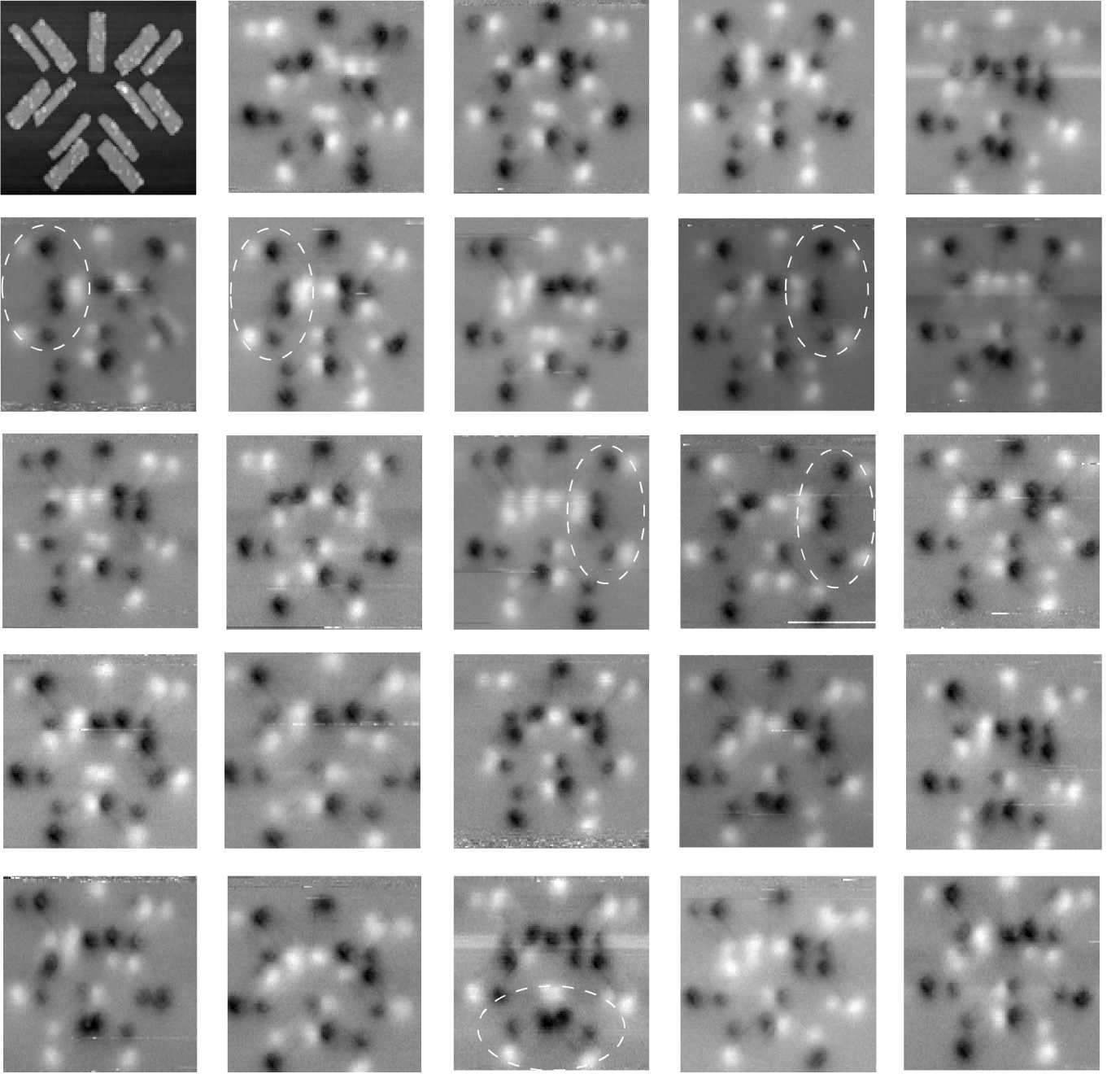


FIG. S8. Magnetic force microscopy (MFM) data on a 24 T-junction set-ups using three Dragonfly's. Top left: Atomic force microscopy (AFM) of one T-junction setup with three dragonfly magnet configurations. Magnetic film height 20 nm. Dashed ovals point out magnetizations favorable for generating MZM. The magnetic history was a magnetizing field from 100 mT to -16 mT to 0 mT applied at 45 degree direction, then 100 mT to -16 mT to 0 mT at 135 degrees.

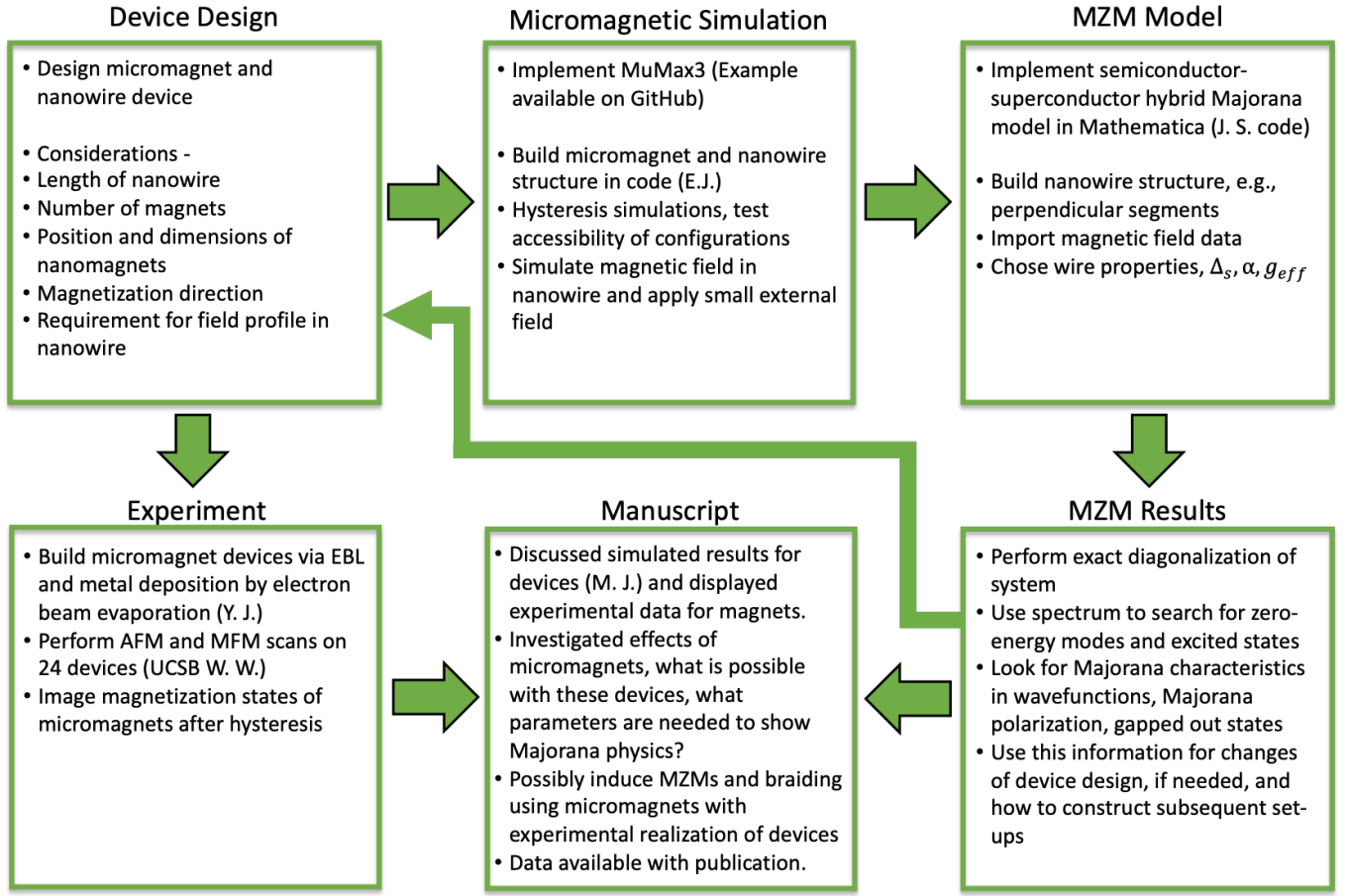


FIG. S9. **Study design, Volume and Duration of study.** The bulk of the this work was carried out over nine months to find an appropriate micromagnet and nanowire set-up that demonstrated MZMs in the hybrid model. Approximately 5 different single Dragonfly configurations were tested and simulated, which was then used to construct the double Dragonfly and the T-junction. There were around 10 different designs tested for the double Dragonfly and T-junction. The experimental data was collected on a single chip where 24 devices had AFM and MFM measurements taken after an hysteresis cycle was applied to magnetize the configurations.